

PROTOSTELLAR DISKS: FORMATION, FRAGMENTATION, AND THE BROWN DWARF DESERT

CHRISTOPHER D. MATZNER^a AND YURI LEVIN^b

^aDepartment of Astronomy & Astrophysics

^bCanadian Institute for Theoretical Astrophysics

University of Toronto, 60 St. George Street, Toronto, ON M5S 3H8, Canada

Draft version November 4, 2018

ABSTRACT

We argue that gravitational instability of typical protostellar disks is not a viable mechanism for the fragmentation into multiple systems – binary stars, brown dwarf companions, or gas giant planets – except at periods above roughly 20,000 years. Our conclusion is based on a comparison between prior numerical work on disk self-gravity by Gammie (2001) with our own analytical models for the dynamical and thermal state of protostellar disks. For this purpose we first develop a simple theory for the initial conditions of low-mass star formation, accounting for the effect of turbulence on the characteristic mass, accretion rate, and angular momentum of collapsing cores. We also present formulae for the probability distribution of these quantities for the case of homogenous Gaussian turbulence. However, our conclusions are not sensitive to this parameterization.

Second, we examine the criterion for fragmentation to occur during star formation, concentrating on the self-gravitational instabilities of protostellar accretion disks in their main accretion phase. Self-gravitational instabilities are strongly dependent on the thermal state of the disk, and we find that the combination of viscous heating and stellar irradiation quenches fragmentation due to Toomre’s local instability. Simulations by Matsumoto & Hanawa (2003), which do not include detailed thermal evolution, predict fragmentation in an early phase of collapse. But, fragments born in this phase are on tight orbits and are likely to merge later due to disk accretion. Global instability of the disk may be required to process mass supply, but this is also unlikely to produce fragments. We conclude that numerical simulations which predict brown dwarf formation by disk fragmentation, but which do not account for irradiation, are unrealistic. Our findings help to explain the dearth of substellar companions to stellar type stars: the brown dwarf desert.

1. INTRODUCTION

At birth, stars accumulate their material through disks that are well known to be dense and massive. Both of these properties make protostellar accretion disks susceptible to self-gravitational instability (e.g., Toomre 1964). Indeed, simulations of protostellar disk accretion and evolution like those of Lin & Pringle (1990) typically find that they approach or cross the threshold for instability, either because of a high disk density or because of a finite disk mass. When this occurs, disk motions caused by self-gravity become important and perhaps dominant sources of angular momentum transport (Paczynski 1978; Lin & Pringle 1987; Papaloizou & Savonije 1991; Adams et al. 1989; Tohline 1994; Laughlin & Bodenheimer 1994; Gammie 2001). Indeed, they may be required for disks to process mass accretion.

Disk self-gravity is of interest not only as a trans-

port mechanism, but also because it may cause the disk to fragment into self-gravitating bodies that can become stellar, substellar, or possibly planetary companions to the star being formed.

If fragments form sufficiently early and survive as most of the stellar mass is accumulated, they stand a chance of acquiring mass comparable to that of the primary object (Bonnell 1994; Matsumoto & Hanawa 2003). Alternatively, fragments that survive but fail to accumulate material may wind up with brown dwarf or planetary masses at the end of accretion, depending partly on where in the disk they form. The possibility that gas giant planets form from fragmentation of a gaseous disk was suggested by Cameron (1978) and advocated by Boss (e.g., Boss 1997). It has been investigated numerically by Mayer et al. (2002), for example. However, numerical investigations are difficult, both because of the high resolution required to attain convergence in self-gravitating simulations of cooling gas (Truelove et al.

1997), and because of the importance of thermal evolution to disk fragmentation (Nelson et al. 2000; Gammie 2001; Pickett et al. 2003; Rafikov 2004). We return to disks’ thermal evolution below.

The possibility that disk instability can produce stellar or substellar companions makes it relevant to the problem of binary and multiple star formation, and to the origin of the stellar initial mass function. The binary problem is reasonably well-posed, since the prestellar cores have been mapped (e.g., Benson & Myers 1989) and binary stars are also well studied. Indeed, binaries’ angular momenta are similar to cores’ (Duquennoy & Mayor 1991; Boss et al. 2000), a fact that explains some trends in binary properties (Fisher 2004). However the mechanism by which a core fragments is currently unclear. It is not understood, for instance, why some stars – albeit less than half – form on their own.

Tohline (2002) has reviewed theories for the origin of binary stars, and identified three leading mechanisms: “prompt” fragmentation in a sheet formed from the quasi-homologous collapse of a cold, rotating cloud; fission of a rapidly rotating and contracting protostar, and self-gravitational instabilities of accretion disks. (Hoyle’s 1953 proposal of opacity limited fragmentation during collapse appears unlikely, due to pressure gradients caused by central concentration of the initial state.) One should add to Tohline’s list *turbulent* fragmentation, in which nonlinear perturbations in the initial state engender fragments directly; see Padoan & Nordlund (2002), Klein et al. (2003), Klessen (2001), and Bate et al. (2003).

This paper will consider axisymmetric models of low-mass star formation. Given the turbulent character of the molecular clouds from which stars form, one might wonder how relevant axisymmetric models can possibly be to stellar fragmentation. However, the energy in this turbulence is concentrated in its longest wavelengths (Larson 1981). The direct progenitors of single and binary stars are the dense molecular cores which are supported significantly by thermal pressure, unlike the larger structures that contain them – their parent cloud or the cloud substructures known as clumps – which are supported entirely by turbulence and magnetic fields (McKee et al. 1993). On the scale of an individual prestellar core, perturbations with longer wavelength appear as translational motion, shear, and overall compression. All of these can be treated with an axisymmetric model in the center of mass frame. Motions with smaller wavelengths constitute turbulence within the core and contribute to turbulent fragmentation but are weaker in general and are suppressed by ion-neutral friction (Zweibel & Josafatsson 1983). For these reasons, and for analytical convenience, we will concentrate on ax-

isymmetric initial conditions.

In this paper we develop a simple prescription for the initial conditions of star formation and examine the susceptibility of the predicted protostellar accretion disks to several modes of gravitational fragmentation. We begin by modeling the effect of molecular cloud turbulence on the masses, radii, and rotation rates of the prestellar molecular cores (§ 2). We then address the “prompt” instability that occurs early in the collapse (§ 3), using criteria developed by the numerical survey of Matsumoto & Hanawa (2003). This analysis suggests that fragmentation occurs quite frequently in the early collapse. However, we argue that this may be an artifact of approximations made in the thermal evolution of core material, and that the fragments so formed are destined to merge during subsequent accretion.

We then turn (§ 4) to fragmentation due to Toomre (1964)’s instability. Since this is governed by the local density, we will call it “local fragmentation”. Here we must discriminate between conditions in which Toomre’s instability saturates, inducing angular momentum transport (Paczynski 1978; Lin & Pringle 1987; Papaloizou & Savonije 1991; Laughlin & Bodenheimer 1994; Laughlin & Rozyczka 1996), and conditions that lead to local fragmentation. For this we rely on Gammie (2001), who identifies the boundary between saturated “gravitoturbulence” and fragmentation in his simulations of razor-thin accretion disks. Although protostellar disks are hardly razor-thin, Gammie’s criterion is a useful litmus test for fragmentation. It demonstrates that the outcome of gravitational instability is sensitive to the thermal evolution of the disk midplane, which we model first by treating only viscous heating alone in §4.1.1. This analysis indicates the possibility of fragments forming with periods greater than about 460 years. However when we account for irradiation from the central star in §4.2, we will demonstrate that this quenches local fragmentation in the main accretion phase, at least for periods up to $\sim 1.2 \times 10^4$ years.

Lastly we treat instability that arises from the finite disk mass (Adams et al. 1989; Tohline 1994). This sets in if other transport mechanisms fail to flush the disk, and Bonnell (1994) suggests it may lead to binary fragmentation. However, current evidence from numerical simulations (Laughlin et al. 1998; Laughlin & Rozyczka 1996) shows that the instability would always redistribute the disk material to quench itself, and the fragmentation would never occur via this channel.

We draw conclusions in §6.3 about the implications of this work for understanding the brown dwarf desert, i.e., the observed underrepresentation of sub-

solar companions to solar type stars.

2. STAR FORMATION: INITIAL CONDITIONS

Prior to their collapse, molecular cores are partially supported by thermal pressure and are confined by the hydrostatic pressure of their parent cloud and permeated by its turbulent motions. Combined with the scalings known to apply to molecular cloud turbulence, these statements suffice to predict, if only crudely, the initial conditions for star formation. See also McKee (1999) and McKee & Tan (2003).

First, consider the structure of cores prior to their collapse. In the absence of non-thermal pressure from magnetic fields, turbulence, or rotation, these are Bonnor-Ebert (BE; Bonnor 1956) spheres, confined by some external pressure P . They exhibit a sequence of increasing self-gravity and central concentration, leading up to a critical state whose mass and radius satisfy

$$M_{\text{BE}} = 1.18 \frac{\sigma_{\text{th}}^4}{G^{3/2} P^{1/2}} \quad \text{and} \quad \frac{M_{\text{BE}}}{R_{\text{BE}}} = 2.43 \frac{\sigma_{\text{th}}^2}{G}, \quad (1)$$

where σ_{th} isothermal sound speed. Molecular line cooling and dust radiation typically conspire to maintain $\sigma_{\text{th}} \simeq 0.2$ km/s, corresponding to temperatures $T \simeq 10$ K for molecular gas (Fuller & Myers 1993); however one can imagine other possibilities, such as star formation in strongly heated or metal-free gas, in which T could be significantly higher.

Because non-thermal forms of pressure also contribute, it is reasonable to replace σ_{th} with an effective sound speed c_{eff} derived below. The Bonnor-Ebert parameters M_{BE} and R_{BE} provide fiducial values for the core mass and radius, although the actual values (M_c and R_c , say) differ because $c_{\text{eff}} > \sigma_{\text{th}}$. We show below that thermal and nonthermal contributions are comparable in these objects.

Goodman et al. (1993) and Burkert & Bodenheimer (2000) have shown that the observed rotation rates of molecular cores are consistent with the turbulent velocity fields of their parent clouds, if extrapolated to the sizes of individual cores. It follows that σ_{NT} for an individual core can be predicted the same way.

Unlike cores, molecular clouds are supported by a triumvirate of turbulent velocity, turbulent magnetic fields (which together compose σ_{NT}) and magnetic field pressure, with σ_{th} being entirely negligible on scales above R_c . Clouds are famously reported to obey a line width-size relation, noted first by Larson (1981) and refined by Solomon et al. (1987), in which

$$\sigma_{\text{NT}}(R)^2 \simeq 0.70 G \Sigma_{\text{cl}} R, \quad (2)$$

corresponding to a state of strong self-gravity (McKee 1999). In eq. (2), R refers to the scale on which σ_{NT} is measured – on the core scale, σ_{NT} would be $\sigma_{\text{NT}}(R_c)$.

The column density of the parent cloud or molecular clump is Σ_{cl} ; Solomon et al. (1987) find, using a virial analysis, that for giant molecular clouds Σ_{cl} is remarkably constant around the value $165 M_{\odot}/\text{pc}^2$. However, Σ_{cl} does depend on context: in M33, for example, Rosolowsky et al. (2003) derive $\Sigma_{\text{cl}} \simeq 120 M_{\odot}/\text{pc}^2$; in the LMC, Pak et al. (1998) derive $\Sigma_{\text{cl}} \sim 700 M_{\odot}/\text{pc}^2$ (± 0.3 dex); and in Galactic clumps forming massive stars (Plume et al. 1997; McKee & Tan 2003) or in extragalactic starburst regions (e.g., Sargent & Scoville 1991; Scoville et al. 1991), $\Sigma_{\text{cl}} \sim 3000 - 5000 M_{\odot}/\text{pc}^2$.

The confining pressure for a core must derive from the mean hydrostatic pressure of the parent clump or cloud; this is (McKee 1999)

$$P = 0.51 f_p G \Sigma_{\text{cl}}^2. \quad (3)$$

where we have included f_p to account for variations in clump or cloud structure (0.51 refers to a spherical cloud with $\rho \propto 1/r$ and no embedded stars) and for fluctuations around the mean value due to turbulence or location within the cloud. With equations (1), this implies

$$\begin{aligned} M_{\text{BE}} &= 1.65 \frac{\sigma_{\text{th}}^4}{f_p^{1/2} G^2 \Sigma_{\text{cl}}} = \frac{0.70}{f_p^{1/2}} \frac{165 M_{\odot} \text{pc}^{-2}}{\Sigma_{\text{cl}}} T_{\text{eff},10}^2 M_{\odot}, \\ R_{\text{BE}} &= 0.68 \frac{\sigma_{\text{th}}^2}{f_p^{1/2} G \Sigma_{\text{cl}}} = \frac{0.034}{f_p^{1/2}} \frac{165 M_{\odot} \text{pc}^{-2}}{\Sigma_{\text{cl}}} T_{\text{eff},10} \text{pc} \end{aligned} \quad (4)$$

where $T_{\text{eff},10}$ is the temperature for which $\sigma_{\text{th}} = c_{\text{eff}}$, measured in units of 10 K.

We wish to highlight two points about Bonnor-Ebert spheres confined by the ambient pressure (equations [1] and [3]) and bathed in turbulence described by equation (2). First, note that the column density of the core is similar to that of the parent cloud or clump:

$$\frac{M_{\text{BE}}}{\pi R_{\text{BE}}^2} = 1.1 f_p^{1/2} \Sigma_{\text{cl}}, \quad (5)$$

independently of σ_{th} . This results from the fact that both the core and the region in which it is embedded are self-gravitating objects whose pressures follow equation (3), and also from the fact that the core's mean pressure is proportional to its surface pressure. McKee & Tan (2003) find a relation quite similar to eq. (5) for turbulence-supported cores.

Second, compare $\sigma_{\text{NT}}(R_{\text{BE}})$ to σ_{th} :

$$\frac{\sigma_{\text{NT}}(R_{\text{BE}})}{\sigma_{\text{th}}} = \frac{0.69}{f_p^{1/4}}. \quad (6)$$

independently of Σ_{cl} . Equation (2) implies that any cloud substructure whose column density is comparable to Σ_{cl} (i.e., any self-gravitating substructure) is suffused with turbulence at the virial level. Extrapolated to the scale of a Bonnor-Ebert sphere, which is assumed to be supported by thermal pressure, this implies $\sigma_{\text{NT}} \simeq \sigma_{\text{th}}$ as in equation (6). Heuristically, the hydrostatic cloud or clump pressure P , which is nonthermal on scales above R_{BE} , must be continuous with the core pressure, which is largely thermal.

Equation (6), in turn, implies that nonthermal motions must be included in the support of cores. To be specific, we adopt¹

$$c_{\text{eff}}^2 = \sigma_{\text{th}}^2 + 1.06\sigma_{\text{NT}}^2 \quad (7)$$

motivated by McKee & Holliman (1999)'s analysis of the mass of regions supported by Alfvén waves (treated in the WKB approximation: McKee & Zweibel 1995). With this, equation (6) is solved if

$$\sigma_{\text{NT}} \simeq \frac{0.98}{f_p^{1/2}} \sigma_{\text{th}}, \quad T_{\text{eff}} \simeq \frac{2.02}{f_p^{1/2}} T_c, \quad (\text{cores}) \quad (8)$$

which are power-law fits to the algebraic solution (good to 20% for $0.5 < f_p < 3$). Cores are therefore somewhat larger than objects lacking turbulent support:

$$M_c \simeq \frac{4.1}{f_p} M_{\text{BE}} = \frac{2.8}{f_p^{3/2}} \frac{165 M_{\odot} \text{pc}^{-2}}{\Sigma_{\text{cl}}} T_{10}^2 M_{\odot},$$

$$R_c \simeq \frac{2.0}{f_p^{1/2}} R_{\text{BE}} = \frac{0.069}{f_p} \frac{165 M_{\odot} \text{pc}^{-2}}{\Sigma_{\text{cl}}} T_{10} \text{ pc} \quad (9)$$

These values are more consistent with observations than R_{BE} and M_{BE} , which points to the presence of turbulent support. The fact that M_c exceeds the mean stellar mass is no concern: Matzner & McKee (2000) have shown that low-mass stars form at an efficiency $\varepsilon \simeq 25\% - 80\%$, due to the action of protostellar winds. Bear in mind, moreover, that there is a mass spectrum of cores going to larger and smaller masses, which generally resembles in its shape the stellar initial mass function (Motte et al. 1998).

It is also worth stressing that the objects we call ‘‘cores’’ are only the smallest and most thermally-supported self-gravitating regions identifiable within molecular clouds. The clumps that form clusters of stars, and clouds themselves, have $\sigma_{\text{NT}} \gg \sigma_{\text{th}}$ and masses much greater than M_c .

We have not yet specified the distribution of the variable f_p that determines cores’ bounding pressures

¹The coefficient of σ_{NT}^2 in eq. (7) depends on how c_{eff} is used. For Alfvén waves treated as a gas with adiabatic index 3/2 and polytropic index 1/2, this coefficient is 3/2 for $P = \rho c_{\text{eff}}^2$ (McKee & Zweibel 1995), 2/3 for $M_{\text{BE}} = 1.18 c_{\text{eff}}^3 / [G^{3/2} \rho(\text{edge})^{1/2}]$ (McKee & Holliman 1999), and 1.06 for $M_{\text{BE}} = 1.18 c_{\text{eff}}^4 / (G^{3/2} P^{1/2})$.

in comparison to the cloud or clump mean pressure. This is a product of several factors: the distribution of pressure within a cloud; the distribution of pressure with time due to turbulent fluctuations; and the likelihood of forming an unstable core, which presumably biases the distribution to higher pressures. On the other hand, the f_p distribution is strongly constrained if one posits that stars always form from marginally stable, thermally-supported cores whose masses are given by equation (9). In that case, the stellar initial mass function is a direct consequence of the core mass distribution: $M_c \propto \varepsilon f_p^{-3/2}$. Conversely, the distribution of f_p is empirically determined, in such a theory, by the distribution of stellar (and binary) masses. For instance, Padoan et al. (1997) attribute the stellar initial mass function to the statistical distribution of pressure in simulations of supersonic, isothermal, unmagnetized turbulence. We will not adopt this strategy for the distribution of f_p , however, for two reasons. First, such a theory predicts that the most massive stars form in the lowest-density regions, which contradicts observations. Second, cores that create massive stars are significantly more massive than M_{BE} and therefore highly turbulent (e.g., McKee & Tan 2003). We reiterate that we consider only the typical, low-mass cores, for which thermal support is naturally significant.

We have not considered static magnetic fields in our treatment of cores; we comment on this in §2.4.

2.1. Core Rotational Properties

We follow Burkert & Bodenheimer (2000) and Fisher (2004) in assuming that the velocity field is homogeneous and Gaussian random with a spectrum consistent with equation (2). These authors also assume the components of \mathbf{v} to be uncorrelated, reducing the mean vorticity relative to an incompressible velocity field of the same σ . We shall first adopt the assumption of uncorrelated velocity components, then consider how the result should be modified to account for gas pressure.

Because both σ_{NT} and the specific angular momentum j derive from \mathbf{v} , one expects $j \propto R_c \sigma_{\text{NT}}(R_c)$, with statistical fluctuations about this scaling. This expectation is borne out in Appendix A, where we compute the full distribution of j . Equations (A19) and (A20) imply, for a velocity field with uncorrelated components,

$$j = 0.34 f_j R_c \sigma_{\text{NT}}$$

$$= 2.3 \times 10^{21} f_j \left(\frac{\Sigma_{\text{cl}}}{165 M_{\odot} \text{pc}^{-2}} \right)^{1/2} \left(\frac{R_c}{0.1 \text{ pc}} \right)^{3/2} \frac{\text{cm}^2}{\text{s}}$$

$$\simeq 1.3 \times 10^{21} \frac{f_j}{f_p^{3/2}} T_{10}^{3/2} \frac{165 M_\odot \text{pc}^{-2} \text{cm}^2}{\Sigma_{\text{cl}}} \frac{\text{cm}^2}{\text{s}} \quad (10)$$

where the last line uses R_c from equation (9).

Since we have assumed \mathbf{v} to be scale free, f_j is chosen from a distribution that depends only on the internal structure of the core, the turbulent spectral slope, and any correlations between components of \mathbf{v} . As explained in §A.2, j is distributed as a Maxwellian, or, crudely,

$$\log_{10} f_j = 0_{-0.49}^{+0.16}. \quad (11)$$

The above results pertain to velocity fields with strictly uncorrelated components, which is not entirely realistic. An uncorrelated flow can be decomposed into an irrotational, potential, compressive portion and a vortical, incompressible portion. In Fourier space, potential flows are aligned with the wavevector and vortical flows are perpendicular to it. Since there are twice as many degrees of freedom in the perpendicular direction, an uncorrelated flow contains two-thirds of its power in vortical motion and one-third in potential flow. Since core angular momentum derives entirely from the vortical part of the flow, it is $\sqrt{3/2}$ times higher in incompressible turbulence as compared to uncorrelated turbulence of the same σ . Equation (8) implies turbulent Mach numbers of about unity on the core scale, suggesting behavior intermediate between the incompressible and pressureless limits. It is reasonable, therefore, to multiply f_j by 1.11 (the harmonic mean of $\sqrt{3/2}$ and unity) to account for correlations introduced by pressure. This correction is however rather minor.

2.2. Collapse of Cores

Cores collapse with the accretion rate characteristic of any self-gravitating body, $\dot{M} = c_{\text{eff}}^3/G$ (Shu 1977). We assume only a fraction ε of the core successfully accretes, so the final stellar mass is $M = \varepsilon M_c$, and

$$\begin{aligned} \dot{M}_{\text{acc}} &\simeq \varepsilon \frac{c_{\text{eff}}^3}{G} \\ &= \frac{2.8 \times 10^{-6}}{f_p^{3/4}} \frac{\varepsilon}{60\%} T_{10}^{3/2} M_\odot \text{yr}^{-1}. \end{aligned} \quad (12)$$

There exists an initial phase of more rapid accretion during which the central region of the core collapses homologously; however, equation (12) is valid for most of the mass.

The theory predicting $\varepsilon \sim 25\% - 80\%$ (Matzner & McKee 2000) invokes the removal of material from the rotational axis by protostellar jets; this somewhat increases the mean angular momentum of accreting material, but we make no correction for this effect.

It is important to note that equation (12) relies on the assumption that cores are the mass reservoir for stars and collapse in their entirety. This accounts neither for the possibility that accretion might be aborted before the collapse has finished (e.g., Reipurth & Clarke 2001), nor for the possibility that accretion continues after the core has collapsed (Bonnell et al. 2001). These effects would alter the amount, duration, and angular momentum of accreted material; however, we assume they can be neglected when estimating the characteristic scales of star formation.

The characteristic disk radius formed during infall is $j^2/(GM)$, or

$$R_d \simeq \frac{f_j^2}{45\varepsilon f_p^{1/2}} R_c = 230 T_{10} \frac{f_j^2}{f_p^{3/2}} \frac{60\%}{\varepsilon} \frac{165 M_\odot \text{pc}^{-2}}{\Sigma_{\text{cl}}} \text{AU}. \quad (13)$$

This is comparable to the critical radius beyond which the disk's self-gravity can cause local fragmentation, at least in principle; see equation (31) below. The maximum disk period is of order 9000 years, but is quite sensitive to the parameters f_j , ε , and f_p .

The inverse relation between R_d and ε results from the fact that a decrease in ε does not reduce the specific angular momentum j of accreted material. This is true for the Matzner & McKee (2000) model, in which an outflow removes material only along the rotational axis. In scenarios where $\varepsilon < 1$ because accretion is aborted, the disk inherits only low- j material from the core center and R_d (and the tendency to fragment) are accordingly suppressed.

2.3. Comparison to Prior Models

We have not attempted to model the internal structures of cores under the influence of both thermal and nonthermal support, as previous authors have done (Myers & Fuller 1992; McKee & Holliman 1999; Curry & McKee 1999). Our emphasis has instead been on the overall mass, radius, and angular momentum scales of the smallest collapsible objects that can exist in a given turbulent environment. For this we rely on a Bonnor-Ebert model, rescaled to account for nonthermal support, and neglect the flattening of the density profile this nonthermal pressure should provide. Although far from perfect, this approximation is best for the most thermally-supported cores on which we concentrate.

In our study of core rotation we have followed Burkert & Bodenheimer (2000) in positing a homogeneous turbulent velocity field obeying the line width-size relation (2) that pervades cores and gives them rotation. Studies of core internal structure have often assumed instead that the nonthermal pressure is a function of the local density, e.g., in constructing

multi-pressure polytrope (McKee & Holliman 1999) or nested polytrope (Curry & McKee 1999) core models, or that it is a function of the local distance from the core’s center (Myers & Fuller 1992). Polytropic models are motivated, in part, by the polytropic behavior of Alfvén wave pressure in the WKB approximation (McKee & Zweibel 1995). This is an idealization because of the predominance of long-wavelength perturbations and because numerical simulations (e.g., Stone et al. 1998; Mac Low 1999) indicate that Alfvén waves damp rapidly in molecular cloud conditions. Our assumption of homogeneous turbulence is equally idealized: it does not explain the origin of the turbulent field, and it ignores the existence of a line width-density relation. We also have not accounted for the possibility of a break in the line width-size relation on scales between the core and its parent clump or cloud. Nevertheless, our results are in reasonable agreement with observations (§2.4).

Our model is similar in some ways to the TNT (thermal plus nonthermal) model introduced by Myers & Fuller (1992) and used recently by McKee & Tan (2003). However the TNT model posits a nonthermal line width that depends on the local radius from the core center: it is akin to the polytropic models in that it associates turbulence with the local conditions. The TNT model also idealizes core density structures as singular power laws, rather than accounting for the flat central region that exists prior to collapse: this is significant because it implies that thermal pressure will always dominate within some radius. In contrast, our models argue for comparable thermal and nonthermal contributions even in maximally thermal cores.

Our predictions for the mass and radius of precollapse cores, equations (9), are similar to those of the smallest (thermal) cores in McKee & Tan (2003)’s theory. However these authors do not account for the possibility of a minimum level of turbulent support. As a result, their thermal cores are less massive and more slowly accreting than we would predict. Although Myers & Fuller and McKee & Tan do not address the core angular momentum distribution, their thermal cores would be significantly more quiescent and more slowly rotating than the cores modeled here.

2.4. Comparison to Observations

Masses: The mass and radius scales derived in §2 (eq. [9]) are consistent with the typical properties of prestellar cores observed in nearby star-forming regions, like Orion B (Johnstone et al. 2001). The core mass spectrum in such surveys typically shows a

power law to masses above the minimum thermally-supported mass identified in this section.

Nonthermal linewidths: Jijina, Myers, & Adams (1999) classified presellar cores according to their association with cores and *IRAS* sources. In their database, those cores that are truly starless in this comparison have median ratios of nonthermal to thermal linewidths about 35% smaller than suggested by equation (8) – see their figure 4. The observed distribution overlaps our prediction. Some of the discrepancy may be attributable to rotational motions that do not contribute to the (beam-resolved) linewidth, or to static magnetic fields.

Jijina, Myers, & Adams observe a correlation between the thermal and nonthermal linewidths: $\sigma_{\text{NT}} \propto \sigma_{\text{th}}^{3.83}$ (their figure 7 and table B7). At the cold and quiescent end of this correlation are L1498 and L1517B, studied in detail by Tafalla et al. (2004). This trend is not explained in our theory, in which equation (8) gives $\sigma_{\text{NT}} \simeq \sigma_{\text{th}}$.

Recall however that equation (8) only represents the characteristic scales of cores. It relies on several assumptions: 1. that the core is at the brink of collapse; 2. that it is free of magnetic support; and 3. that it has the minimum level of turbulence consistent with assumptions 1 and 2 in the context of a homogeneous model for the turbulent velocity field. An individual core need not adhere to these assumptions, although we have argued that they suffice to set characteristic scales. In the case of the very quiescent cores² L1498 and L1517B, we suspect that magnetic fields rather than turbulence are supplying a significant amount of nonthermal support.

Nonthermal support: Johnstone et al. (2001) identify an effective temperature, using Bonnor-Ebert, models which is typically 20-40 K. Many of these clumps’ actual temperatures measured at less than 20 K, with 10 K being typical. A significant contribution of nonthermal pressure – as in our equation (8) – offers an explanation for this discrepancy.

It is interesting to note that this level of nonthermal support holds even in the very quiescent cores L1498 and L1517B, for which Tafalla et al. (2004) find $T_{\text{eff}} = 28$ and 20 K, respectively, in their Bonnor-Ebert fits. Compared to the measured thermal temperatures $T_c = 10$ and 9.5 K, we note that the ratio is consistent with equation (8) although the linewidths are not. Although part of the nonthermal support of these cores is rotational, most is likely magnetic.

Rotation rates: As for core rotation rates, equation (10) agrees with the value $j \sim 10^{21} \text{ cm}^2 \text{ s}^{-1}$ deduced by Goodman et al. (1993) for cores of similar mass. The second line differs from Burkert & Bodenheimer (2000)’s formula $j = 7 \times 10^{20} (R_c/0.1\text{pc})^{3/2} \text{ cm}^2 \text{ s}^{-1}$.

²These are not characteristic of the 172 Jijina, Myers, & Adams (1999) cores: for instance, L1498 is their smallest core.

However, Burkert & Bodenheimer’s results were numerical; our own unpublished numerical experiments, which were based on their method, exhibit a bias to underestimate j by about the same factor. We believe this arises due to the periodic boundary conditions employed in the numerical grid; due to limited dynamical range, these impose correlations on the box scale that affect the spectrum as sampled on the core scale and smaller.

The rotation rates observed by Tafalla et al. (2004) for the very quiescent cores L1498 and L1517B are only a factor of a few smaller than the typical values predicted by equation (10), and are within the distribution described by equation (11).

Accretion rates: Motoyama & Yoshida (2003) review a range of observational evidence that mass accretion can significantly exceed the characteristic value c_s^3/G in an early (class 0) accretion phase. They suggest the initial phase of homologous collapse, or collapse induced by an external impulse (see also Hennebelle et al. 2003), as possible explanations. These possibilities are both very reasonable, but note that we predict an accretion rate of roughly $2.6c_s^3/G$, on account of the nonthermal support (eq. [12]). Therefore, the need to invoke alternative explanations for the observed protostellar accretion rates is partially alleviated.

Magnetic fields: Finally, we comment on the neglect of static magnetic fields in our calculations. Employing the Chandrasekhar-Fermi method, Crutcher et al. (2004) find that static magnetic fields in prestellar cores could either be subdominant or comparable in magnitude with thermal pressure, depending on the application of a geometrical correction factor to their observations. Theoretically, one expects that ambipolar diffusion will sap the influence of magnetic fields prior to core collapse. In addition, inferences of short core lifetimes (e.g., Visser et al. 2002) and observations of high core column densities (Nakano 1998) are taken to indicate that static magnetic fields are not significant in core support. On theoretical grounds, Zweibel & Josafatsson (1983) find that ambipolar diffusion is accelerated in turbulent gas. We conclude that our approximation of zero mean field is adequate given current uncertainties, while recognizing that this should be re-examined in future work. As discussed above, magnetic fields may be especially important for understanding the thermal-nonthermal linewidth correlation seen by Jijina, Myers, & Adams (1999) and the nonthermal support of quiescent cores seen by Tafalla et al. (2004).

The first opportunity for fragmentation is in the initial phase of collapse, which follows from the homologous contraction of the core’s central region. In this phase, the mass accretion rate can exceed equation (12). If the core’s central region rotates sufficiently rapidly, it will form a disk that can fragment.

This phase of fragmentation has been studied in detail recently by Matsumoto & Hanawa (2003), who consider the initial collapse of slowly rotating Bonnor-Ebert spheres. Matsumoto & Hanawa find that fragmentation occurs by one mode or another so long as $\Omega_c t_{\text{ff,ctr}} \gtrsim 0.045$, where Ω_c is the rotation rate and $t_{\text{ff,ctr}}$ is the free-fall time evaluated at the middle of the initial state. Using equations (9), (10), and the moment of inertia $I_c = 0.2827M_c R_c^2$, we find

$$\Omega_c t_{\text{ff,ctr}} \simeq 0.25 \frac{f_j}{f_p^{1/4}}. \quad (14)$$

By this criterion, then, all but the most slowly rotating cores ($f_j < 0.18f_p^{1/4}$; about 3% of the population according to eq. [A20]) should undergo fragmentation in the initial collapse phase.

However, this conclusion is not robust. Note, first, that Matsumoto & Hanawa (2003) rely on the approximation of barotropic core collapse (isothermal, for $n_H < 10^{13} \text{ cm}^{-3}$) rather than a detailed thermodynamic calculation. Boss et al. (2000) caution that protostellar collapse simulations employing the Eddington approximation differ significantly with regard to fragmentation from those that use a barotropic law. Recently, Larson (2004) has argued that thermal evolution plays a critical role in determining stellar masses. Likewise, numerical and analytical studies of disk fragmentation (Gammie 2001; Pickett et al. 2003; Rafikov 2004; Levin 2003) stress the importance of cooling. We will return to this issue in detail in §4 and add some comments in §6.2.

Second, Matsumoto & Hanawa’s calculations stop after at most $0.07M_\odot$ of several M_\odot have accreted into fragments. As they point out, the future evolution of these fragments is difficult to predict. We note that the remaining mass accretes through a disk around the newly formed objects. The specific angular momentum of this material greatly exceeds that of the observed fragments. As shown by Bate & Bonnell (1997), a binary tightens due to gravitational interaction with the circumbinary disc. We suspect that this drives prompt protostellar fragments to merge. Future simulations will be required to test this hypothesis, especially for the complicated case of multiple prompt fragmentations. If prompt fragmentation *does* succeed, it should produce tight binaries with j significantly below the typical value cited in equation (10) – an therefore, significantly below the median of the binary distribution (Duquennoy & Mayor 1991).

For both of these reasons we take equation (14) to be only *suggestive* of fragmentation in the initial, impulsive collapse phase. We probe fragmentation in later stages of accretion in the upcoming sections.

4. STEADY PROTOSTELLAR DISKS: LOCAL GRAVITATIONAL INSTABILITY AND LOCAL FRAGMENTATION

We now explore the stability of the steady protostellar accretion disks that form during the collapse of cores like those described in §2, during the phase of main accretion during which the accretion rate is given by (12). There are two modes by which self-gravitation can trigger disk fragmentation, one of which is subject to a local instability criterion (Toomre 1964) and the other a global one (Shu et al. 1990). We focus initially on the local instability and return to the global one in §5. The consequences of Toomre’s instability have been greatly elucidated by the numerical simulations of Gammie (2001), as described below.

Lin & Pringle (1990) have carried out an analysis of protostellar disk evolution, based on initial conditions qualitatively similar to those sketched in §2. They implemented a gravitational viscosity that rose as Toomre’s instability parameter,

$$Q \equiv \frac{c_d \Omega}{\pi G \Sigma}, \quad (15)$$

declined through its critical value of unity. Here Ω and Σ are the disk’s orbital frequency and column density, respectively; and

$$c_d \equiv \sqrt{\frac{\partial \int_{-\infty}^{\infty} P dz}{\partial \Sigma}}$$

(where z is altitude) is the signal speed in the disk, which is slightly above the midplane isothermal sound speed $c_s \equiv \sqrt{P/\rho}$. With this prescription for angular momentum transport, they found Q saturating typically in the range 0.2-0.5. This study lacked, however, two physical important physical effects: 1. the nonlocal nature of gravitational angular momentum transport when $Q > 1$; and 2. the dissolution into fragments of disks with $Q \lesssim 1$. Both shortcomings are addressed by the nonlinear simulations of Laughlin et al. (1998) and Gammie (2001):

1. When gravitational instability is weak and $Q > 1$, spiral modes saturate at low amplitudes via mode-mode coupling (Laughlin et al. 1998); in this state, redistribution of angular momentum is nonlocal and is described only approximately by a local prescription, i.e., by Shakura & Sunyaev’s α parameter. On

the other hand, strongly unstable disks enter a state of “gravitoturbulence” (Gammie 2001) in which the coherence length is only a few effective scale heights

$$H \equiv \frac{c_s}{\Omega}.$$

In this state angular momentum transport is a local process (see also Lodato & Rice 2004). At the brink of fragmentation, Shakura & Sunyaev’s viscosity parameter α takes maximal value, which Gammie (2001) shows to be³

$$\alpha = \frac{4}{9(\gamma_{2d} - 1)\Omega t_{\text{cool}}} \quad (16)$$

if t_{cool} is the cooling timescale in the critical state.

We recall that α is related to the mass accretion rate through the disk:

$$\dot{M}_{\text{visc}} = \frac{3\pi\alpha\Sigma c_s^2}{\Omega}. \quad (17)$$

The subscript “visc” is added to distinguish the accretion rate due to local viscous transport from, for instance, the rate of mass supply (eq. [12]).

Goodman (2003) points out that angular momentum loss in magnetized winds can lead mass to accrete more rapidly than equation (16) predicts. We however assume that strong winds do not develop over most of the disk radius, and we adopt equation (16) as a maximal value.

2. By identifying the precise boundary between gravitoturbulent and fragmenting disks, Gammie (2001) provides the means to discriminate stable mass accretion from the formation of new bound objects. A number of papers argue that the precise outcome of fragmentation depends sensitively on the thermal properties of the disk (e.g., Pickett et al. 2003); nevertheless the threshold for instability is given adequately by equation (20).

These insights reveal two points about Lin & Pringle’s simulations. First, they estimate in a reasonable fashion the dynamics of protostellar disks in their main accretion phase (since their estimate of α approximates Gammie’s result when $Q = 1$); and second, that these disks are close enough to $Q = 1$ to merit an careful investigation of whether fragmentation does indeed occur.

The results of Gammie’s two-dimensional simulations (corroborated in three dimensions by Rice et al. 2003) provide a practical, local description for the disks that have entered a state of self-gravitating turbulence. This state separates disks that are relatively smooth from those that have fragmented into swarms

³We define α using the isothermal sound speed c_s , rather than the disk signal speed c_d , in equation (17). As a result our α differs by a factor γ_{2d} relative to its definition in Gammie (2001).

of clumps; it also is a state in which the mean midplane conditions (density, temperature, etc.) are reasonably constrained. We use it as a litmus test for fragmentation in a variety of circumstances.

4.1. Local criteria for fragmentation by Toomre's instability

Toomre (1964) demonstrated the onset of axisymmetric instability in disks with $Q < 1$; although other modes grow for somewhat higher Q , Gammie (2001) verified that $Q \simeq 1$ at the boundary of fragmentation.

To assess whether the disk can process accretion without fragmenting, we adopt

$$c_d^2 = \gamma_{2d} c_s^2, \quad \text{where} \quad \gamma_{2d} \equiv \frac{\partial \ln \int_{-\infty}^{\infty} P dz}{\partial \ln \Sigma} \quad (18)$$

in equations (15) and (16). In the limits of weak self-gravity (Goldreich et al. 1986) or strong self-gravity (Gammie 2001), respectively,

$$\gamma_{2d} = \begin{cases} \frac{3\gamma-1}{\gamma+1} & (Q \gg 1) \\ 3 - \frac{2}{\gamma} & (Q \ll 1) \end{cases} \quad (19)$$

where γ is the adiabatic index of disk gas.

Gammie (2001) adopted the specific value $\gamma_{2d} = 2$, corresponding to $\gamma = 3$ or 2 for strong or weak self-gravity, respectively. Either value is stiffer than a realistic disk. In the temperature range of interest, a protostellar disk obeys $\gamma = 5/3$ because rotational degrees of freedom are not excited;⁴ then $\gamma_{2d} = 3/2$ or $9/5$ in the strong and weak self-gravity limits, respectively. At the onset of fragmentation $Q \simeq 1$, and we assume that

$$\gamma_{2d} \simeq 1.65, \quad (Q = 1)$$

an intermediate value. We also assume that the critical cooling time remains roughly one half orbital period, i.e., $\Omega t_{\text{cool}} = 3$, for the softer equation of state; this remains to be checked by future numerical experiments. With these choices, equation (16) gives

$$\alpha = 0.23. \quad (Q = 1) \quad (20)$$

Weak and strong self-gravity give $\alpha = 0.30$ and 0.19 , respectively. We adopt $\alpha = 0.23$ as a fiducial maximal value, but consider this uncertain by about 50%.

The condition $Q = 1$ may immediately be expressed in terms of c_s , the midplane density ρ , and the midplane pressure p :

$$c_s = \frac{\pi G \Sigma}{\gamma_{2d}^{1/2} \Omega}, \quad \rho = \frac{\gamma_{2d}^{1/2} \Omega^2}{2\pi G}, \quad \text{and} \quad p = \frac{\pi}{2\gamma_{2d}^{1/2}} G \Sigma^2 \quad (21)$$

⁴Shock heating and radiative transfer alter the effective γ from its adiabatic value, especially for disks close to fragmentation. However it is the adiabatic γ that enters in the theory of Gammie (2001).

where the middle expression uses the approximate relation $\rho = \Sigma \Omega / (2c_s)$, and the last expression uses $p = \rho c_s^2$. These relations are only approximate, as they neglect the disk's self-gravity in its vertical structure, but they suffice to delineate the onset of instability.

An important additional criterion comes from combining eqs. (12), (15), and (17) to give

$$\frac{\dot{M}_{\text{visc}}}{\dot{M}_{\text{acc}}} = \frac{3\alpha \gamma_{2d}^{1/2} c_s^3}{\varepsilon Q c_{\text{eff}}^3}. \quad (22)$$

Conversely, if the disk processes gas in steady state ($\dot{M}_{\text{visc}} = \dot{M}_{\text{acc}}$) then

$$Q = \frac{3\alpha \gamma_{2d}^{1/2} c_s^3}{\varepsilon c_{\text{eff}}^3}. \quad (\text{steady - state}) \quad (23)$$

Using $\gamma_{2d} = 1.65$ and $\alpha = 0.23$ to describe the onset of fragmentation, we find that the disk can process steady accretion with $Q > 1$ only when

$$c_s > 1.04 \varepsilon^{1/3} c_{\text{eff}}; \quad (24)$$

i.e., using eq. (8) to describe a typical unstable core,

$$T > 1.08 \varepsilon^{2/3} T_{\text{eff}} \simeq \frac{1.56}{f_p^{1/2}} \left(\frac{\varepsilon}{60\%} \right)^{2/3} T_c \quad (25)$$

(where T refers to the midplane temperature); otherwise fragmentation will occur where the gas falls. For typical core temperatures of order 10 K, disks colder than about 15.6 K are unable to process the high accretion rate and will fragment into clumps. This critical temperature is rather insensitive to the uncertainties described after equation (20): it varies as $\alpha^{-2/3} \gamma_{2d}^{-1/3}$.

4.1.1. Self-luminous disks

If the heat generated locally by viscosity is responsible for the midplane temperature, then criterion (24) may be evaluated directly. Our treatment follows Lin & Pringle (1990) and Levin (2003), among others. In thermal steady state, the flux of viscous energy radiated by each face of the disk is related to the accretion rate through

$$F_v = \frac{3\Omega^2 \dot{M}}{8\pi}. \quad (26)$$

The flux can also be derived from radiation transfer across an optical depth $\kappa\Sigma/2$ from the disk midplane to its surface; therefore

$$F_r = \sigma T^4 \times \begin{cases} 4\tau_{\text{PI}} & (\tau \ll 1) \\ 8/(3\tau_{\text{R}}) & (\tau \gg 1) \end{cases} \quad (27)$$

where $\tau_{\text{R,PI}} = \kappa_{\text{R,PI}}\Sigma/2$ is the optical depth corresponding to Rosseland or Planck opacity, κ_{R} or κ_{PI} , respectively.⁵ The factor 16/3 arises in the optically thick case when the dissipation rate per unit mass is a constant (e.g., Chick & Cassen 1997) and is only approximate. For the disk to achieve an equilibrium temperature in which local heating balances radiative cooling, we must have $F_v = F_r$.

The midplane temperature and sound speed are related via

$$c_s^2 = \frac{k_B T}{\mu} \quad (28)$$

where $\mu \simeq 2.3m_p$ is the mean molecular weight. We neglect the radiation pressure in this expression. This is entirely justified for present-day star formation, since when $Q = 1$ the ratio of gas to radiation pressure is

$$\frac{3k_B\Omega^2}{2\pi G a \mu T^3} = 11 \left(\frac{1000 \text{ yr}}{\text{period}} \right)^2 \left(\frac{500 \text{ K}}{T} \right)^3$$

using eq. (21).

For the opacity we adopt

$$\begin{pmatrix} \kappa_{\text{R}} \\ \kappa_{\text{PI}} \end{pmatrix} = \kappa_0 T^2 = \begin{pmatrix} 3.0 f_{\kappa_{\text{R}}} \\ 8.4 f_{\kappa_{\text{PI}}} \end{pmatrix} \times 10^{-4} T^2 \text{ cm}^2 \text{ g}^{-1}. \quad (29)$$

This describes the ice branch of Semenov et al. (2003)'s ice grain opacities in their ‘‘composite aggregate’’ model; eq. (29) fits their results around 16 K. Note that Alexander & Ferguson (1994) computed somewhat lower opacities ($f_{\kappa_{\text{R}}} \simeq 0.67$; see also Bell & Lin 1994). Henning & Stognienko (1996) also derive a lower value ($f_{\kappa_{\text{R}}} \simeq 0.43$) after allowing for dust agglomeration in the parent molecular core. We include the two f_{κ} factors to account for variations in metallicity, dust processing, and uncertainties in opacity modeling.

Equations (26), (27), (28), and (29) provide enough information to solve $F_v = F_r$ for $T(r)$, given an accretion rate \dot{M} . As discussed above, the local accretion rate (eq. [17]) must match the supply (eq. [12]). To determine the onset of fragmentation, we also impose

⁵Recently, Johnson & Gammie (2003) have published numerical experiments on razor-thin discs and have shown that Eq. (27) is generally inaccurate when the disc develops strong gravitationally-driven turbulence. However, in their model the breakdown of Eq. (27) is serious when the opacity is a sensitive function of temperature, which occurs only when the dust begins to evaporate at above 1000 K. Temperatures this high are clearly irrelevant for protostellar discs beyond a fraction of an AU, and thus for the problem at hand Eq. (27) is adequate. We also note that when the opacity is temperature sensitive, then the one-zone model of Johnson & Gammie does not treat faithfully the vertical radiative transport in a real disc.

$Q \rightarrow 1$ (eq. [15]). We find that fragmentation ensues when

$$\Omega = \Omega_{\text{cr}} \times \begin{cases} \left(\frac{c_{\text{eff}}}{c_s} \right)^{10}, & c_s < c_{s,\tau} \ (\tau \ll 1) \\ 1, & c_s > c_{s,\tau} \ (\tau \gg 1) \end{cases} \quad (30)$$

where

$$\begin{aligned} \Omega_{\text{cr}} &= 3.60 \left[\frac{G^2 \mu^2 \sigma}{\alpha \kappa_0 \gamma_{2d} k_B^2} \right]^{1/3} \\ &= \frac{4.3 \times 10^{-10}}{f_{\kappa_{\text{R}}}^{1/3}} \left(\frac{\mu}{2.3m_p} \right)^{2/3} \left(\frac{0.23}{\alpha} \frac{1.65}{\gamma_{2d}} \right)^{1/3} \text{ s}^{-1}, \end{aligned} \quad (31)$$

corresponding to a period of 460 years for the fiducial parameters (400 years for Alexander & Ferguson's opacity; 350 years for Henning & Stognienko's opacity), and

$$\begin{aligned} c_{s,\tau} &= \frac{0.174}{f_{\kappa_{\text{R}}}^{1/30} f_{\kappa_{\text{PI}}}^{1/10}} \left(\frac{\alpha}{0.23} \right)^{1/15} \left(\frac{1.65}{\gamma_{2d}} \right)^{1/30} \\ &\quad \times \left(\frac{2.3m_p}{\mu} \right)^{8/15} \text{ km s}^{-1}. \end{aligned} \quad (32)$$

To summarize, disks with opacity law (29) that are warmed solely by their own viscosity will be subject to local fragmentation in any region whose orbital frequency is less than the value given in eq. (30).

It is worthwhile to emphasize two points about the above equations. First, Ω_{cr} is an upper bound for the frequency of a locally unstable disk, i.e., all locally unstable disks have periods of roughly 460 years or longer. This bound depends *only* on the opacity law of the disk midplane and is independent of the mass supply rate and disk surface density (so long as the disk is optically thick). This result is specific to a cancellation that occurs when the opacity varies as T^2 .

Second, the lower bound on the period at which fragmentation can occur is pushed to even higher values if the disk is optically thin or if it is affected by external irradiation. The division between optically thin and thick fragmentation depends only on the midplane sound speed c_s ; the critical value $c_{s,\tau}$ corresponds to a midplane temperature of roughly 8.4 K. But recall that the fragmentation temperature is determined by the mass supply rate to be roughly $T \simeq 16$ K for cores with $T_c = 10$ K (eq. [25]). This implies that disks are typically optically thick

at the fragmentation bound. Indeed, using equations (25) and (32), all cores with

$$T_c > 5.4 \frac{f_p^{1/2}}{f_{\kappa\text{Pl}}^{1/5} f_{\kappa\text{R}}^{1/15}} \left(\frac{60\%}{\varepsilon} \right)^{2/3} \text{ K} \quad (33)$$

will produce disks that are significantly more prone to fragmentation than those from colder cores because of the transition to optically thick disks. (In equation [33], we suppress the variation $T_c \propto \alpha^{4/5} \gamma_{2d}^{4/15} \mu^{-1/15}$ around fiducial values of these parameters.)

Equation (30) argues strongly against the formation of giant planets by direct disk fragmentation, in agreement with the recent work by Rafikov (2004). This argument gains strength when the effect of stellar irradiation is considered.

Fragment masses. We pause here to note the characteristic masses of fragments formed by local gravitational instability. This topic is investigated in detail by Levin (2003) and Goodman & Tan (2004). If fragments form, their initial mass is of order $\Sigma(2\pi H)^2$, i.e., roughly Jupiter's mass for both the optically thick and optically thin cases if $T_c = 10$ K (but scaling as $T_c^{3/2}$ and $T_c^{-7/2}$ respectively). Continued growth is likely up to the gap-opening mass, which we estimate at 36 Jupiter masses for fiducial parameters, and perhaps beyond. Local fragmentation is therefore most relevant to the origin of planetary (Boss 1997) or brown dwarf (Bate et al. 2002) companions.

4.2. Irradiation

The preceding section identified a critical midplane temperature for local fragmentation (typically ~ 15.6 K in disks around low-mass protostars, eq. [25]), and a critical disk period (typ. ~ 460 yr) above which viscous heating permits cooler midplane temperatures. However as we mentioned before, the argument in the preceding section neglects external irradiation of the disc. Here we self-consistently take irradiation into account and show that it completely prevents local fragmentation for a wide range of core parameters.

To illustrate its importance, suppose irradiation normal to the disk surface is a fraction f_F of the spherical flux. The equilibrium temperature of an optically thick disk is then given by $\sigma T^4 = f_F L / (4\pi R_d^2)$, if L is the accretion luminosity; or

$$94 f_F^{1/4} \left(\frac{T_\star}{4500} \right)^{1/3} \left(\frac{460 \text{ yr}}{\text{period}} \right)^{1/3} \left(\frac{\dot{M}_{\text{acc}}}{2 \times 10^{-6} M_\odot \text{ yr}^{-1}} \right)^{1/6} \text{ K} \quad (34)$$

where the stellar effective temperature is T_\star . (Note this is independent of the stellar mass M , if referenced to orbital period.) If the disk is optically

thin, its temperature is generically higher than given above: for a local radiation energy density is aT_{egy}^4 and color temperature is T_c , the equilibrium temperature T of an optically thin region is

$$T^4 \kappa_{\text{Pl}}(T) = T_{\text{egy}}^4 \kappa_{\text{Pl}}(T_c) \quad (35)$$

where κ_{Pl} refers to the Planck average opacity. Since $\kappa_{\text{Pl}}(T)$ is monotonic in the temperature range of interest, $T_{\text{egy}} < T < T_c$. Furthermore, since the flux at the disk surface cannot exceed $aT_{\text{egy}}^4 c$, an optically thin disk must be warmer than a thick disk in the same radiation environment.⁶

The flux suppression factor f_F can be quite small in the case that the disk is illuminated at a grazing incidence from the stellar photosphere (e.g., Kenyon & Hartmann 1987; Chiang & Goldreich 1997). For an accreting protostar, however, reradiation from the stellar envelope tends to illuminate and heat the disk (Keene & Masson 1990; Natta 1993; Chick et al. 1996; Chick & Cassen 1997; D'Alessio et al. 1997).

To gauge this, consider the column of the infall envelope. The spherically averaged column density outward from some radius r is $\Sigma_{\text{sph}}(r) = \dot{M} / [2\pi r v_{\text{esc}}(r)]$. Evaluated at the centrifugal radius in eq. (13),

$$\Sigma_{\text{sph}}(R_d) = 0.43 \frac{\varepsilon}{60\%} \frac{f_p^{3/4}}{f_j} \Sigma_{\text{cl}}. \quad (36)$$

In spherical infall $\Sigma_{\text{sph}}(r)$ diverges inward as $r^{-1/2}$. For rotating infall, however, only low- j material persists within R_d ; this makes $\Sigma_{\text{sph}}(R_d)$ a characteristic value for the column *inward* from R_d , as well.

Intriguingly, the characteristic column $\Sigma_{\text{sph}}(R_d)$ is roughly $\Sigma_{\text{cl}}/2$, i.e., half that of the parent clump or cloud, at the end of accretion. (Beforehand it is much greater: the column to the disk edge varies as t^{-2} during steady accretion.) Deviations from spherical symmetry due to angular momentum are given by the rotating-infall solution of Terebey, Shu, & Cassen (1984). Additionally, the protostellar jet will scour the axis to produce a cavity.

Since star formation appears to be limited to regions of high visual extinction (Onishi et al. 1998; Hara et al. 1999; Johnstone et al. 2004, as suggested theoretically by McKee 1989), and since $\Sigma_{\text{sph}}(R_d) \simeq \Sigma_{\text{cl}}/2$, starlight is absorbed and reprocessed after it traverses a fraction of the infall column. This reprocessing is strongly affected by the presence or absence of an outflow cavity: therefore, we consider both cases below.

⁶The lower limit on T in the thin case is $\sqrt{2}$ below that in eq. (34), but this factor is not significant.

The temperature of an irradiated disk depends on the optical depth of the disk to the incoming radiation and to its own thermal emission. For a disk at the fragmentation threshold with $Q = 1$,

$$\begin{aligned} \frac{\Sigma(R_d)}{\Sigma_{\text{sph}}} &= \frac{3\alpha}{2^{3/2}} \left(\frac{H}{r}\right)^2 \\ &= 210 \frac{f_p^{1/2}}{f_j^2} \left(\frac{\varepsilon}{60\%}\right)^{4/3}. \end{aligned} \quad (37)$$

The first line derives from equations (15), (18), (24), and (36); the second line applies the results of §2 (and varies as $(\gamma_{2d}/\alpha)^{1/3}$ around our fiducial values). The outer disk column is thus of order 90 Σ_{cl} , or ~ 3 g cm^{-2} for typical clouds. According to the opacity law (29), the disk will be vertically optically thick to Planck radiation of color temperature exceeding

$$19.6 \frac{f_j^{3/2}}{f_{\kappa\text{P1}}^{1/2} f_p^{5/8}} \left(\frac{165 M_\odot \text{pc}^{-2}}{\Sigma_{\text{cl}}}\right)^{1/2} \text{ K}.$$

The disk's opacity to radiation from dust of a certain temperature is higher than to a Planck field of that color temperature: $f_{\kappa\text{P1}} \simeq 2.5$ for dust radiation. This lowers the critical illuminating temperature to about 12 K, and oblique illumination lowers it further still. The disk can therefore be assumed optically thick to irradiation, although it is only marginally thick with respect to its own radiation at a fragmentation temperature of ~ 15.6 K.

4.2.1. No outflow cavity

The reprocessing radius typically lies well inside R_d but outside the dust evaporation radius, because the latter is optically thin in the end phases of accretion. Disk irradiation is therefore due primarily to the second reprocessing of starlight at radii around R_d . We shall identify the dust temperature at the reprocessing surface, which affects the amount of re-absorption and re-emission above the disk.

Close to the protostar, the angle-averaged column density in the Terebey, Shu, & Cassen (1984) infall profile is $\bar{\Sigma}(r) = 1.17(r/R_d)^{1/2}\Sigma_{\text{sph}}(R_d) + \mathcal{O}(r/R_d)^{3/2}$. We identify the reprocessing radius r_1 with the surface of optical depth unity, then $\bar{\Sigma}(r_1)\kappa_\star = 1$, where $\kappa_\star \equiv \kappa_{\text{P1}}(T_\star)$ is the opacity to starlight of color temperature T_\star . In addition, equation (35) determines the dust temperature T_1 at this location: $\kappa_{\text{P1}}(T_1)T_1^4 = \kappa_\star L/(4\pi r_1^2 ac)$. Combining these,

$$\frac{\kappa_{\text{P1}}(T_1)}{\kappa_\star^5} \sigma T_1^4 = \frac{L\Sigma_{\text{sph}}^4}{26.7}. \quad (38)$$

⁷ T_1 also depends weakly on the gas density at r_1 , which affects the evaporation temperatures of the dust components; this is ignored in eq. 38.

The left hand side is a somewhat complicated function of T_1 because the dust composition, a function of T_1 , determines κ_\star and $\kappa_{\text{P1}}(T_1)$; metallicity and the stellar temperature T_\star also enter.⁷ The right hand side depends on model parameters. A self-consistent solution of (38) is not always available; this signals a change in the dust composition and fixes T_1 at a composition boundary. Nevertheless, this equation demonstrates that the reprocessing temperature T_1 is a pure function of $L\Sigma_{\text{sph}}^4$ for fixed T_\star and metallicity, so long as the infall is optically thick to starlight. In a range of T_1 for which the dust composition is constant, $T_1 \propto L^{1/6}\Sigma_{\text{sph}}^{2/3}$ because $\kappa_{\text{P1}}(T_1) \propto T_1^2$.

Given a optically thin emission at the reprocessing temperature T_1 , the effective opacity for the second reprocessing event is given by

$$\bar{\kappa} = \frac{\int \kappa_{\nu 2} \kappa_{\nu 1} B_\nu(T_1)}{\int \kappa_{\nu 1} B_\nu(T_1)} \quad (39)$$

where $\kappa_{\nu 1}$ is the opacity law at the reprocessing radius and $\kappa_{\nu 2}$ is that for cool dust near R_d . Figure 1 shows T_1 and $\bar{\kappa}$ for a given model; notably, $\bar{\kappa} \simeq 15$ $\text{cm}^2 \text{g}^{-1}$ for a wide range of parameters, dropping only for especially large disk radii (and especially low values of $\Sigma_{\text{sph}}(R_d)$).

Integrating the flux through the disk at R_d from the sky intensity of reradiated light (assuming optically thin second reprocessing), we find that the flux of this radiation at the disk radius R_d is given by equation (34) if

$$f_F = 0.28\bar{\kappa}\Sigma_{\text{sph}} \quad (40)$$

giving $f_F \simeq 1/16$ for typical parameters. Using this result to calculate the irradiation temperature of an optically *thick* disk in eq. (34), we find that it falls below the critical temperature for local fragmentation at the outer disk edge only if

$$\begin{aligned} \text{period} &> \frac{7400 f_p^{1.69}}{f_j^{3/4}} \left(\frac{\bar{\kappa}}{10 \text{ cm}^2 \text{g}^{-1}} \frac{\Sigma_{\text{cl}}}{165 M_\odot \text{pc}^{-2}}\right)^{3/4} \\ &\times \left(\frac{T_\star}{4500 \text{ K}}\right) \left(\frac{10 \text{ K}}{T_c}\right)^{9/4} \text{ yr} \end{aligned} \quad (41)$$

there; this is comparable to the characteristic maximum period in §2.2.

Note we have taken $\varepsilon = 100\%$ here, since the absence of the outflow cavity implies that all of the material is accreted onto the star. This raises the critical disk temperature to about 22 K.

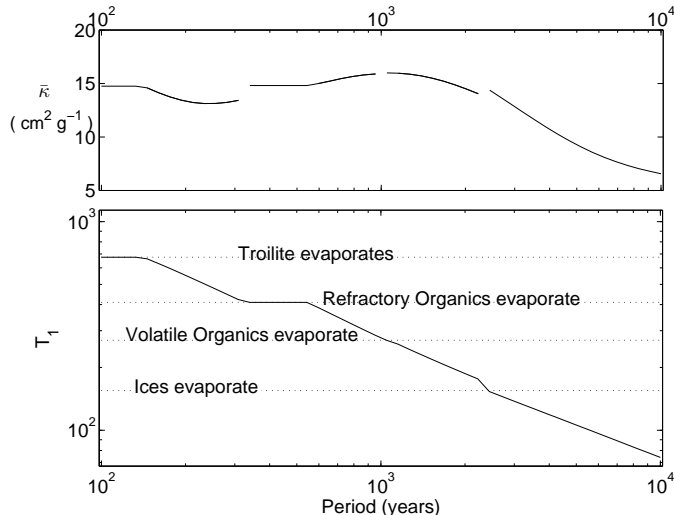


FIG. 1.— Lower panel: Temperature T_1 of the reprocessing surface in envelopes lacking outflow cavities. T_1 is computed as a function of outer disk period using the opacity model of Semenov et al. (2003). Assumed parameters are $M = 0.5M_\odot$, $\dot{M} = 3 \times 10^{-6} M_\odot \text{ yr}^{-1}$, $T_\star = 4500 \text{ K}$, and solar metallicity; however, equation (38) permits this diagram to be rescaled for other parameters. (The density dependence of evaporation temperatures has been suppressed for simplicity; lines here are drawn for $10^{-10} \text{ g cm}^{-3}$.) Upper panel: effective opacity $\bar{\kappa}$ of cool dust to optically thin thermal radiation from dust of temperature T_1 .

4.2.2. Outflow cavity

A more realistic calculation must account for the region along the axis that is cleared by the jet. An outflow cavity warms the disk by providing more direct illumination than is available otherwise. To calculate this we must specify the shape of the outflow cavity.

Note, first, that the wind ram pressure is expected generically to vary as $1/(r^2 \sin^2 \theta)$ with distance and angle θ from the axis (Matzner & McKee 1999). Inflow ram pressure scales as $r^{-5/2}$ from the centrifugal radius to the edge of the inflow. We see on comparison that inflow dominates close to the star and near the equator, and the wind dominates far from the star and near the axis. By this reasoning, Matzner & McKee (2000) divided the initial core into accreting and ejected angles depending on the velocity imparted by the wind impulse to gas at the edge of the core. Our parameter ε is simply the accreted mass as a fraction of the initial mass.

By the same logic, gas that is not cast away by the wind is destined to fall inward, and its motion is less and less affected by the wind ram pressure as it does. Therefore we are justified in approximating the shape of the outflow cavity as an unperturbed streamline in the infall solution of Terebey, Shu, & Cassen (1984). The streamline in question is roughly the one that divides infall and outflow in Matzner & McKee (2000)'s theory. For the case of a spherical initial core, then, the initial angle of this streamline is given by

$$\cos \theta_0 = \varepsilon. \quad (42)$$

(We shall assume a spherical core for the remainder of this section.) This streamline strikes the disk at a radius $\sin^2(\theta_0)R_d = (1 - \varepsilon^2)R_d$.

Geometrically, a fraction ε of the starlight strikes the cavity inner edge because the remaining $1 - \varepsilon$ is cleared by the outflow. However, smaller ε leads to a broader outflow cavity, which causes a greater portion of the reprocessed starlight to reach the disk. After performing ray-tracing calculations of reradiation from the inner edge of the infall, using a geometry like that shown in figure 2, we find that f_F is adequately described by $0.1\varepsilon^{-0.35}$ in the relevant range $20\% < \varepsilon < 90\%$. The infall envelope is translucent to this reprocessed radiation, but our estimates indicate that shadowing of the disk by the infall is insufficient to change this result significantly.

The disk's edge is too hot to fragment unless

$$\text{period} > 2.4 \times 10^4 f_p^{9/8} \left(\frac{60\%}{\varepsilon} \right)^{1.8} \frac{T_\star}{4500 \text{ K}} \left(\frac{10 \text{ K}}{T_c} \right)^{9/4} \text{ yr}. \quad (43)$$

Consider now the evolution of the effect of irradiation as the accretion rate declines. The critical disk midplane temperature, eq. (25), varies as $\dot{M}_{\text{acc}}^{2/3}$. The radiative flux normal to the outer disk varies as the central luminosity ($\propto \dot{M}_{\text{acc}}$ for low-mass stars); if the infall is optically thin then there is another factor of \dot{M}_{acc} in the reprocessed fraction. The flux therefore varies as $\dot{M}_{\text{acc}}^{1-2}$, implying a midplane temperature that varies as $\dot{M}_{\text{acc}}^{0.25-0.5}$. The weaker dependence implies that a disk which is stabilized by irradiation will remain so as the mass supply wanes. This might

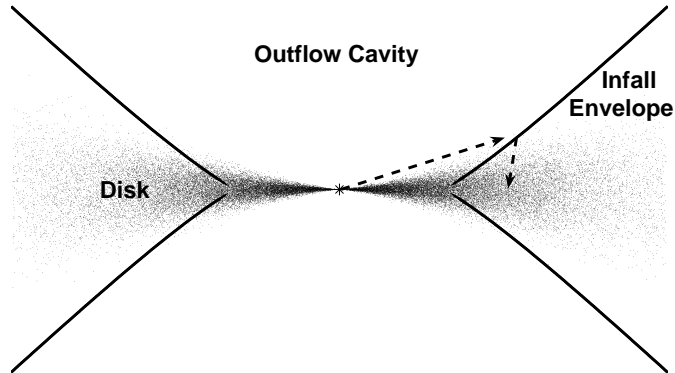


FIG. 2.— A schematic diagram for irradiation in the presence of an outflow cavity, in the theory of §4.2.2. The inflow envelope is excavated within a particular streamline (eq. [42], solid line); visible starlight is absorbed near this innermost streamline and reprocessed into infrared light that illuminates the disk (dashed arrows).

not hold if accretion were to stop suddenly compared to the disk’s viscous time, but this is not realistic.

To summarize, *local fragmentation due to Toomre’s instability is quenched by irradiation in protostellar disks*, in all but exceptionally long-period systems whose orbital separations are of order 1000 AU.

However, disks fragment at smaller periods if they form from cores that are warmer than 10 K or from more turbulent cores than were described in §2. Disks around massive stars fall in this category (McKee & Tan 2003), although their central illumination is different than we have assumed.

5. GLOBAL INSTABILITY

In light of the previous section, one expects irradiation to prevent local fragmentation and possibly also to prevent the enhanced angular momentum transport from self-gravity. Note, however, that Gammie (2001)’s results were for razor-thin disks, and protostellar disks are rather thick in comparison. Therefore, the disk mass can become large enough to induce global instability. As we shall see, the threshold for this depends on the ability of local angular momentum transport (e.g., due to MRI) to remove material from the disk.

Adams et al. (1989) and Shu et al. (1990) describe a global “SLING” instability in which the disk becomes massive enough that the star is perturbed from the center of mass by the action of a lopsided spiral. Shu et al. (1990) provide the following formula (their eq. [111]) for the criterion of instability:

$$\frac{M_d}{M_d + M} = \frac{3}{4\pi} \mathcal{M}(Q) \quad (44)$$

where

$$\begin{aligned} \mathcal{M}(Q) &\equiv \int [x^4 + 4Q^2(x - x^{5/2})]^{1/2} dx \\ &\simeq 1 + \frac{8}{9}(Q - 1) \end{aligned} \quad (45)$$

where the approximation is exact in the limits $Q \rightarrow 1$ and $Q \rightarrow \infty$ and holds within 2.3% for all $Q > 1$. When it sets in, this instability is thought to transport material rapidly enough to prevent fragmentation (Laughlin et al. 1998, see however Bonnell 1994).

We shall not posit $Q = 1$, because we have seen in §4.2 that irradiation tends to warm the disk so that $Q > 1$. Instead, let us assume $\Sigma \propto r^{-3/2}$ so that $M_d = 4\pi R_d^2 \Sigma$. If we approximate $\Omega^2 \simeq G(M + M_d)/R_d^3$ and retain $H = c_s/\Omega$, then (15) becomes

$$Q = 4 \frac{H}{r} \left(1 + \frac{M}{M_d} \right). \quad (46)$$

With equations (44) and (45), this gives a maximum stable disk mass as a function of H/r . We find that $Q > 1$ and $M_d < M$ requires $0.06 < H/r < 0.28$; within this range, we approximate the exact solution of equations (44), (45), and (46):

$$\frac{M_d}{M} < 3.09 \frac{H}{r} + 0.13 \quad (47)$$

for global stability. The approximation is valid within 1%.

This can be compared to the mass accumulated, which for $\Sigma \propto r^{-3/2}$ is

$$M_d = \frac{\dot{M}_{\text{acc}}}{\Omega} \frac{4}{3\alpha} \left(\frac{r}{H} \right)^2. \quad (48)$$

The comparison sets a minimum for α/α_0 , where

$$\alpha_0 \equiv \frac{\dot{M}_{\text{acc}}}{M\Omega}. \quad (49)$$

The theory of §2 indicates that

$$\alpha_0 = 10^{-2.6} \frac{f_j^3}{f_p^{3/4}} \left(\frac{60\%}{\varepsilon} \right)^2, \quad (50)$$

independently of the physical scale of the parent cloud.

Taken together, we find that the minimum α required to keep the disk stable can be approximated (within 4.2%)

$$\alpha > 0.52 \left(\frac{r}{H} \right)^{2.76} \alpha_0. \quad (51)$$

The instability is clearly very sensitive to the mid-plane temperature. Computing $H/r = c_s/v_k$ using the irradiation temperature model of §4.2.2 (which gives $H/r \sim 0.11$ for fiducial parameters), we find that stability requires

$$\alpha > 0.19 \frac{f_j^{1.62}}{f_p^{1.27}} \left(\frac{60\%}{\varepsilon} \right)^{0.27} \left(\frac{T_c}{10 \text{ K}} \right)^{1.27} \times \left(\frac{165 M_\odot \text{ pc}^{-2}}{\Sigma_{\text{cl}}} \right)^{0.46} \left(\frac{4500}{T_\star} \right)^{0.46}. \quad (52)$$

It has been argued that local gravitational transport becomes significant when Q falls below ~ 1.4 (Laughlin & Bodenheimer 1994). In its absence, the disk is left with magnetoturbulent (MRI) transport, which is thought to saturate at much lower values of α in a weakly ionized medium.

With eq. (52), this indicates that global spiral modes *can be* required for protostellar disks to process the mass supply, depending on the infall parameters and on the detailed irradiation temperature (which we have calculated only approximately). Disks that are especially thick or whose parent cores are especially slowly rotating ($f_j \ll 1$) will be stable at smaller values of α .

6. SUMMARY AND CONCLUSIONS

6.1. *Summary*

We derived in §2 a simple set of relations for the smallest and most thermally supported collapsible objects, i.e., cores, that can exist at a given mean gas temperature in a parent cloud of a given column density. The cloud column sets both the scale for the cores' bounding pressure, and the coefficient in the line width-size relation for cloud turbulence. This turbulence aids in core support and increases the minimum core mass, while also accelerating the accretion rate when cores do collapse (§2.2). In addition, turbulence bestows cores with rotational angular momentum that determines the characteristic scales for protostellar accretion disks (§2.1). This theory does not account for the role of a static magnetic field, nor does it prescribe the distribution of overpressures expected in a realistic model for molecular cloud turbulence; nevertheless, it matches the observations of

prestellar cores of a couple solar masses (§2.4) with a minimum of free parameters. In our model, substellar cores would derive from regions of especially low temperature and high degrees of overpressure. High mass cores could come from the opposite conditions or, more likely, derive the bulk of their initial support from nonthermal pressure.

Turning next to the fragmentation boundary as predicted even in axisymmetric models of protostellar collapse, we found in §3 that the cores are typically subject to a phase of prompt fragmentation according to Matsumoto & Hanawa (2003)'s criterion. This is a possible mechanism for the production of relatively tight binary stars. However, we note that this occurs before most of the core mass has accreted; therefore these fragments may be driven to merge by radiating angular momentum to the accretion disk. We also stress that Matsumoto & Hanawa's simulations used an approximation to the thermal evolution of the collapsing core, and that we and others have found the gas temperature to be a controlling physical factor in fragmentation. We therefore do not consider it certain that binaries form by this mechanism.

Examining the local gravitational stability of protostellar disks in §4.1, we made extensive use of the simulations by Gammie (2001) to identify a critical disk temperature that divides accreting from fragmenting disks. For disks heated solely and locally by their own viscosity, we found in §4.1.1 that local fragmentation is impossible for disk periods shorter than about 460 years (depending on the opacity law), and that fragmentation is suppressed until much longer periods if the disk is optically thin to its own cooling radiation. This conclusion is entirely consistent with the recent argument by Rafikov (2004) that the formation of giant planets by direct disk instability (Boss 1997) is impossible on thermodynamic grounds. Moreover, when we account for heating by the star's accretion luminosity (reprocessed by the infall envelope), we find that the local instability is entirely quenched out to very long periods, $\sim 10^{4.1}$ years. A decline in the accretion rate does not alter this conclusion.

Lastly, we consider the onset of global instability due to the accumulation of a finite disk mass. Applying the instability criterion of Shu et al. (1990), we find that the intrinsic viscosity parameter α (e.g., due to MRI) must exceed roughly 0.2 in order to prevent global instability. This makes global instability a primary candidate for angular momentum transport within protostellar disks. When it does occur, this instability is likely to saturate and provide rapid angular momentum transport rather than fragmentation (Laughlin et al. 1998).

6.2. Implications for Numerical Simulations of Multiple Star Formation

Thermal evolution plays a critical role in determining the onset and outcome of gravitational stability in disks (Toomre 1964; Cassen et al. 1981; Tomley et al. 1991, 1994; Pickett et al. 1998, 1999, 2000; Gammie 2001; Pickett et al. 2003). We find that local disk fragmentation is quenched by stellar irradiation except at very large periods (§ 4.2; see also D’Alessio et al. 1997) and, even in the absence of irradiation, inhibited for short periods (< 460 years) by viscous heating (§4.1.1).

These observations are quite important for the interpretation of large-scale numerical simulations designed to predict star formation. Currently, only a few multidimensional calculations have accounted for radiation transfer during collapse (Boss et al. 2000), and then only in an approximate manner. No dynamical simulations have yet included disk irradiation due to starlight that is reprocessed by the infall envelope. Disk fragmentation in these simulations is unlikely to be realistic.

For instance, three quarters of the brown dwarfs formed in the simulations of Bate et al. (2002) arise via disk fragmentation. Since these simulations employ a barotropic equation of state, we predict that these brown dwarfs would not form if stellar irradiation were accounted for.

We have demonstrated in §3 that initial conditions for most collapsing cores are favorable for the prompt fragmentation simulated by Matsumoto & Hanawa (2003). However, since these were also performed with a barotropic equation of state, and since they do not extend long enough to determine whether the fragments will merge, we consider them provisional and await radiation transfer calculations of the same parameter space.

6.3. Conclusions: Stellar Binaries and the Brown Dwarf Desert

Our foremost conclusion is that stellar and substellar companions are not produced by disk fragmentation, except possibly in an early phase of core collapse (although we argue this is unlikely: see §3) or at very large periods of $\sim 10^{4.1}$ years (§4.2). This indicates that turbulent perturbations beyond rotation and compression are responsible for the production of binary stars (Klein et al. 2003; Bate et al. 2002). Since companions formed in disk instabilities would be initially of substellar mass, this closes a formation channel for substellar companions over a wide range of orbital periods. Observations (e.g., McCarthy & Zuckerman 2004) show a marked dearth of companions in the mass range between stars and planets – a brown dwarf desert. Armitage & Bonnell (2002) have ascribed this to inward disk migration that destroys brown dwarfs. However this presupposes that they can form within disks; here we have argued that they cannot.

Barrado y Navascués et al. (2004) argue from their observations of disk accretion onto free-floating brown dwarfs that these must form in isolation rather than from fragmentation in a disk or in a collapsing turbulent core. Our theoretical results also argue against a disk origin for these objects.

We thank Jonathan Williams, Ue-Li Pen, and Fred Adams for helpful and encouraging discussions; Mary Barsony and Sukanya Chakrabarti for useful comments; Roman Rafikov for pointing us to his preprint; and Dmitry Semenov for explanations concerning the Semenov et al. (2003) opacity model. Comments from our anonymous referee have been very helpful in improving the clarity of the paper. CDM’s research is funded by NSERC and the Canada Research Chairs program. YL is supported by an NSERC senior CITA postdoc.

References

- Adams, F. C., Ruden, S. P., & Shu, F. H. 1989, *ApJ*, 347, 959
- Alexander, D. R. & Ferguson, J. W. 1994, *ApJ*, 437, 879
- Armitage, P. J. & Bonnell, I. A. 2002, *MNRAS*, 330, L11
- Barrado y Navascués, D., Mohanty, S., & Jayawardhana, R. 2004, *ApJ*, 604, 284
- Bate, M. R. & Bonnell, I. A. 1997, *MNRAS*, 285, 33
- Bate, M. R., Bonnell, I. A., & Bromm, V. 2002, *MNRAS*, 332, L65
- Bate, M. R., Bonnell, I. A., & Bromm, V. 2003, *MNRAS*, 339, 577
- Bell, K. R. & Lin, D. N. C. 1994, *ApJ*, 427, 987

- Benson, P. J. & Myers, P. C. 1989, *ApJS*, 71, 89
- Bonnell, I. A. 1994, *MNRAS*, 269, 837
- Bonnell, I. A., Bate, M. R., Clarke, C. J., & Pringle, J. E. 2001, *MNRAS*, 323, 785
- Bonnor, W. B. 1956, *MNRAS*, 116, 351
- Boss, A. P. 1997, *Science*, 276, 1836
- Boss, A. P., Fisher, R. T., Klein, R. I., & McKee, C. F. 2000, *ApJ*, 528, 325
- Burkert, A. & Bodenheimer, P. 2000, *ApJ*, 543, 822
- Cameron, A. G. W. 1978, *Moon and Planets*, 18, 5
- Cassen, P. M., Smith, B. F., Miller, R. H., & Reynolds, R. T. 1981, *Icarus*, 48, 377
- Chiang, E. I. & Goldreich, P. 1997, *ApJ*, 490, 368
- Chick, K. M. & Cassen, P. 1997, *ApJ*, 477, 398
- Chick, K. M., Pollack, J. B., & Cassen, P. 1996, *ApJ*, 461, 956
- Crutcher, R. M., Nutter, D. J., Ward-Thompson, D., & Kirk, J. M. 2004, *ApJ*, 600, 279
- Curry, C. & McKee, C. F. 1999
- D'Alessio, P., Calvet, N., & Hartmann, L. 1997, *ApJ*, 474, 397
- Duquennoy, A. & Mayor, M. 1991, *A&A*, 248, 485
- Fisher, R. T. 2004, *ApJ*, 600, 769
- Fuller, G. A. & Myers, P. C. 1993, *ApJ*, 418, 273
- Gammie, C. F. 2001, *ApJ*, 553, 174
- Goldreich, P., Goodman, J., & Narayan, R. 1986, *MNRAS*, 221, 339
- Goodman, A. A., Benson, P. J., Fuller, G. A., & Myers, P. C. 1993, *ApJ*, 406, 528
- Goodman, J. 2003, *MNRAS*, 339, 937
- Goodman, J. & Tan, J. C. 2004, *ApJ*, 608, 108
- Hara, A., Tachihara, K., Mizuno, A., Onishi, T., Kawamura, A., Obayashi, A., & Fukui, Y. 1999, *PASJ*, 51, 895
- Hennebelle, P., Whitworth, A. P., Gladwin, P. P., & André, P. 2003, *MNRAS*, 340, 870
- Henning, T. & Stognienko, R. 1996, *A&A*, 311, 291
- Hoyle, F. 1953, *ApJ*, 118, 513
- Jijina, J., Myers, P. C., & Adams, F. C. 1999, *ApJS*, 125, 161
- Johnson, B. M. & Gammie, C. F. 2003, *ApJ*, 597, 131
- Johnstone, D., Fich, M., Mitchell, G. F., & Moriarty-Schieven, G. 2001, *ApJ*, 559, 307
- Johnstone, D., Di Francesco, J., & Kirk, H. 2004, *ApJ*, 611, L45
- Keene, J. & Masson, C. R. 1990, *ApJ*, 355, 635

- Kenyon, S. J. & Hartmann, L. 1987, *ApJ*, 323, 714
- Klein, R. I., Fisher, R. T., Krumholz, M. R., & McKee, C. F. 2003, in *Revista Mexicana de Astronomia y Astrofisica Conference Series*, 92–96
- Klessen, R. S. 2001, *ApJ*, 556, 837
- Larson, R. B. 1981, *MNRAS*, 194, 809
- Larson, R. B. 2004, *ArXiv Astrophysics e-prints*, astro-ph/0412357
- Laughlin, G. & Bodenheimer, P. 1994, *ApJ*, 436, 335
- Laughlin, G., Korchagin, V., & Adams, F. C. 1998, *ApJ*, 504, 945
- Laughlin, G. & Rozyczka, M. 1996, *ApJ*, 456, 279
- Levin, Y. 2003, *ArXiv Astrophysics e-prints* (astro-ph/0307084)
- Lin, D. N. C. & Pringle, J. E. 1987, *MNRAS*, 225, 607
- . 1990, *ApJ*, 358, 515
- Lodato, G. & Rice, W. K. M. 2004, *MNRAS*, 351, 630
- Mac Low, M.-M. 1999, *ApJ*, 524, 169
- Matsumoto, T. & Hanawa, T. 2003, *ApJ*, 595, 913
- Matzner, C. D. & McKee, C. F. 1999, *ApJ*, 526, L109
- . 2000, *ApJ*, 545, 364
- Mayer, L., Quinn, T., Wadsley, J., & Stadel, J. 2002, *Science*, 298, 1756
- McCarthy, C. & Zuckerman, B. 2004, *AJ*, 127, 2871
- McKee, C. F. 1989, *ApJ*, 345, 782
- McKee, C. F. 1999, in *NATO ASIC Proc. 540: The Origin of Stars and Planetary Systems*, 29
- McKee, C. F. & Holliman, John H., I. 1999, *ApJ*, 522, 313
- McKee, C. F. & Tan, J. C. 2003, *ApJ*, 585, 850
- McKee, C. F. & Zweibel, E. G. 1995, *ApJ*, 440, 686
- McKee, C. F., Zweibel, E. G., Goodman, A. A., & Heiles, C. 1993, in *Protostars and Planets*, 327
- Motoyama, K. & Yoshida, T. 2003, *MNRAS*, 344, 461
- Motte, F., André, P., & Neri, R. 1998, *A&A*, 336, 150
- Myers, P. C. & Fuller, G. A. 1992, *ApJ*, 396, 631
- Nakano, T. 1998, *ApJ*, 494, 587
- Natta, A. 1993, *ApJ*, 412, 761
- Nelson, A. F., Benz, W., & Ruzmaikina, T. V. 2000, *ApJ*, 529, 357
- Onishi, T., Mizuno, A., Kawamura, A., Ogawa, H., & Fukui, Y. 1998, *ApJ*, 502, 296
- Paczynski, B. 1978, *Acta Astronomica*, 28, 91

- Padoan, P. & Nordlund, Å. 2002, *ApJ*, 576, 870
- Padoan, P., Nordlund, A., & Jones, B. J. T. 1997, *MNRAS*, 288, 145
- Pak, S., Jaffe, D. T., Van Dishoeck, E. F., Johansson, L. E. B., & Booth, R. S. 1998, *ApJ*, 498, 735
- Papaloizou, J. C. & Savonije, G. J. 1991, *MNRAS*, 248, 353
- Pickett, B. K., Cassen, P., Durisen, R. H., & Link, R. 1998, *ApJ*, 504, 468
- Pickett, B. K., Cassen, P., Durisen, R. H., & Link, R. 1999, *ASSL Vol. 240: Numerical Astrophysics*, 177
- Pickett, B. K., Cassen, P., Durisen, R. H., & Link, R. 2000, *ApJ*, 529, 1034
- Pickett, B. K., Mejía, A. C., Durisen, R. H., Cassen, P. M., Berry, D. K., & Link, R. P. 2003, *ApJ*, 590, 1060
- Plume, R., Jaffe, D. T., Evans, N. J., I., Martin-Pintado, J., & Gomez-Gonzalez, J. 1997, *ApJ*, 476, 730
- Rafikov, R. 2004, *ArXiv Astrophysics e-prints* (astro-ph/0406469)
- Reipurth, B., & Clarke, C. 2001, *AJ*, 122, 432
- Rice, W. K. M., Armitage, P. J., Bate, M. R., & Bonnell, I. A. 2003, *MNRAS*, 339, 1025
- Rosolowsky, E., Engargiola, G., Plambeck, R., & Blitz, L. 2003, *ArXiv Astrophysics e-prints*
- Sargent, A. & Scoville, N. 1991, *ApJ*, 366, L1
- Scoville, N. Z., Sargent, A. I., Sanders, D. B., & Soifer, B. T. 1991, *ApJ*, 366, L5
- Semenov, D., Henning, T., Helling, C., Ilgner, M., & Sedlmayr, E. 2003, *A&A*, 410, 611
- Shakura, N. I. & Sunyaev, R. A. 1973, *A&A*, 24, 337
- Shu, F. H. 1977, *ApJ*, 214, 488
- Shu, F. H., Tremaine, S., Adams, F. C., & Ruden, S. P. 1990, *ApJ*, 358, 495
- Solomon, P. M., Rivolo, A. R., Barrett, J., & Yahil, A. 1987, *ApJ*, 319, 730
- Stone, J. M., Ostriker, E. C., & Gammie, C. F. 1998, *ApJ*, 508, L99
- Tafalla, M., Myers, P. C., Caselli, P., & Walmsley, C. M. 2004, *A&A*, 416, 191
- Terebey, S., Shu, F. H., & Cassen, P. 1984, *ApJ*, 286, 529
- Tohline, J. E. 1994, in *Physics of Accretion Disks Around Compact and Young Stars*, 9–10
- Tohline, J. E. 2002, *ARA&A*, 40, 349
- Tomley, L., Cassen, P., & Steiman-Cameron, T. 1991, *ApJ*, 382, 530
- Tomley, L., Steiman-Cameron, T. Y., & Cassen, P. 1994, *ApJ*, 422, 850
- Toomre, A. 1964, *ApJ*, 139, 1217
- Truelove, J. K., Klein, R. I., McKee, C. F., Holliman, J. H., Howell, L. H., Greenough, J. A., Howell, L. H., & Greenough, J. A. 1997, *ApJ*, 489, L179+
- Visser, A. E., Richer, J. S., & Chandler, C. J. 2002, *AJ*, 124, 2756
- Zweibel, E. G. 2002, *ApJ*, 567, 962
- Zweibel, E. G. & Josafatsson, K. 1983, *ApJ*, 270, 511

SPECIFIC ANGULAR MOMENTUM DISTRIBUTION OF PRESTELLAR CORES

We now compute the angular momentum distribution quoted in equations (10) and (11) according to the model for core rotation described in §2.1. Specifically, we assume in the present calculation a spatially homogeneous velocity fields \mathbf{v} whose components are uncorrelated Gaussian fields obeying a line width-size scaling like that in equation (2). The effect of gas pressure, which introduces correlations by inhibiting compression, is discussed separately in §2.1. As a consequence of homogeneity, we assume no correlation between \mathbf{v} and the core density field $\rho(r)$. See §2.3 for a discussion of these and alternative assumptions.

Since we are interested in the specific angular momentum normalized to $R\sigma_{\text{NT}}(R)$, we compute j and $\sigma_{\text{NT}}(R)$ separately.

Angular momentum

To satisfy the line width-size relation in this model, we must impose that the velocity difference between the two points scales as a square root of the distance between the points. More precisely,

$$\langle [v_i(r_1) - v_j(r_2)]^2 \rangle = k|\mathbf{r}_1 - \mathbf{r}_2|\delta_{ij} \quad (\text{A1})$$

where we assume that $|r_1 - r_2| \ll v^2/k$ if $v = \langle |\mathbf{v}|^2 \rangle^{1/2}$ is the characteristic turbulent velocity. Here, angle brackets denote an ensemble average over realizations of the turbulent velocity field, or equivalently, over the location of the core within this field. Equation (A1) is assumed to hold for each velocity component v_i independently. Expanding equation (A1),

$$\langle v_i(r_1)v_j(r_2) \rangle = \left(\frac{1}{3}v^2 - \frac{1}{2}k|\mathbf{r}_1 - \mathbf{r}_2| \right) \delta_{ij}. \quad (\text{A2})$$

Skipping to the result, the root mean square angular momentum of a core in this velocity field is given by

$$\langle L^2 \rangle^{1/2} = 2\pi k^{1/2} R^{9/2} \rho_0 [F(\bar{\rho})]^{1/2}, \quad (\text{A3})$$

where R is the core radius and ρ_0 is a reference density; $\bar{\rho}(\bar{r}) = \rho(r)/\rho_0$ is the spherically symmetric normalized density profile expressed in terms of the dimensionless radius $\bar{r} = r/R$, and the form factor F is given by the following double integral:

$$F = \int_0^1 \int_0^1 d\bar{r}_1 d\bar{r}_2 \bar{\rho}(\bar{r}_1) \bar{\rho}(\bar{r}_2) \bar{r}_1 \bar{r}_2 (\bar{r}_1^2 + \bar{r}_2^2)^{5/2} \times \\ \left\{ \frac{1}{5} [(1+q)^{5/2} - (1-q)^{5/2}] - \frac{1}{3} [(1+q)^{3/2} - (1-q)^{3/2}] \right\}. \quad (\text{A4})$$

Here $q = 2r_1 r_2 / (r_1^2 + r_2^2)$.

Evaluated over a Bonnor-Ebert sphere, $F^{1/2} = 0.0294$. Such spheres obey $M = 0.735\rho_0 R^3$, so that

$$\langle j^2 \rangle^{1/2} = \frac{\langle L^2 \rangle^{1/2}}{M} = 0.251 k^{1/2} R^{3/2}. \quad (\text{A5})$$

The derivation is as follows. The total angular momentum is given by

$$L^2 = L_x^2 + L_y^2 + L_z^2. \quad (\text{A6})$$

By spherical symmetry the components of angular momentum are uncorrelated; this can be checked directly. Therefore,

$$\langle L^2 \rangle = 3\langle L_z^2 \rangle = 3\langle (L_1 - L_2)^2 \rangle, \quad (\text{A7})$$

where

$$L_1 = \int d^3\mathbf{r} \rho(r) x v_y, \quad (\text{A8})$$

$$L_2 = \int d^3\mathbf{r} \rho(r) y v_x \quad (\text{A9})$$

But $\langle L_1 L_2 \rangle = 0$ and, by spherical symmetry, $\langle L_1^2 \rangle = \langle L_2^2 \rangle$. Therefore,

$$\begin{aligned} \langle L^2 \rangle &= 6 \langle L_1^2 \rangle \\ &= 6 \int \int d^3 \mathbf{r}_1 d^3 \mathbf{r}_2 \rho(r_1) \rho(r_2) x_1 x_2 \langle v_y(\mathbf{r}_1) v_y(\mathbf{r}_2) \rangle. \end{aligned} \quad (\text{A10})$$

We can now use Eq. (A2) and evaluate the integral above. First, note that only the second term on the right-hand side of Eq. (A2) contributes to the integral. Second, because of the spherical symmetry we can substitute $x_1 x_2$ by $(\mathbf{r}_1 \mathbf{r}_2)/3$ in the integrand. Thus we have for the total angular momentum:

$$\langle L^2 \rangle = -k \int \int d^3 \mathbf{r}_1 d^3 \mathbf{r}_2 \rho(r_1) \rho(r_2) (\mathbf{r}_1 \mathbf{r}_2) |\mathbf{r}_1 - \mathbf{r}_2|. \quad (\text{A11})$$

The integrand in Eq. (A11) depends only on the magnitudes of \mathbf{r}_1 and \mathbf{r}_2 , and on the angle θ between them. Therefore, the other three free variables are integrated out, and we are left with the 3-d integral:

$$\begin{aligned} \langle L^2 \rangle &= -k \int dr_1 4\pi r_1^2 \rho(r_1) \times \\ &\quad \int \int dr_2 2\pi d \cos \theta \cos \theta \left[\rho(r_2) r_1 r_2 \sqrt{r_1^2 + r_2^2} \right. \\ &\quad \left. \sqrt{1 - q \cos \theta} \right], \end{aligned} \quad (\text{A12})$$

where

$$q = \frac{2r_1 r_2}{r_1^2 + r_2^2}. \quad (\text{A13})$$

The angular integration in Eq. (A12) can be performed analytically, most simply by using $\sqrt{1 - q \cos \theta}$ as an integration variable. The result of this calculation is presented in Equations (A3) and (A4).

One-dimensional velocity dispersion

We now compute the one-dimensional velocity dispersion:

$$\begin{aligned} \sigma^2 &= \int d^3 \mathbf{r} \tilde{\rho} [v_x(\mathbf{r}) - \bar{v}_x]^2 \\ &= \int d^3 \mathbf{r} \tilde{\rho} [v_x(\mathbf{r})^2 - 2v_x(\mathbf{r})\bar{v}_x + \bar{v}_x^2] \\ &= \left[\int d^3 \mathbf{r} \tilde{\rho} v_x(\mathbf{r})^2 \right] - \bar{v}_x^2 \end{aligned} \quad (\text{A14})$$

where $\tilde{\rho} \equiv \rho/M$ and \bar{v} denotes the center of mass velocity:

$$\bar{v} = \int d^3 \mathbf{r} \tilde{\rho} v(\mathbf{r}) \quad (\text{A15})$$

In equation (A14), the first term reduces after ensemble averaging to $v^2/3$, according to equation (A2). Likewise for the second term,

$$\begin{aligned} \langle \bar{v}_x^2 \rangle &= \int \int d^3 \mathbf{r}_1 d^3 \mathbf{r}_2 \tilde{\rho}(\mathbf{r}_1) \tilde{\rho}(\mathbf{r}_2) \langle v_x(\mathbf{r}_1) v_x(\mathbf{r}_2) \rangle \\ &= \int \int d^3 \mathbf{r}_1 d^3 \mathbf{r}_2 \tilde{\rho}(\mathbf{r}_1) \tilde{\rho}(\mathbf{r}_2) \left(\frac{1}{3} v^2 - \frac{1}{2} k |\mathbf{r}_1 - \mathbf{r}_2| \right). \end{aligned} \quad (\text{A16})$$

The constant terms cancel in the ensemble average of eq. (A14), leaving

$$\begin{aligned} \langle \sigma^2 \rangle &= \frac{1}{2} k \int \int d^3 \mathbf{r}_1 d^3 \mathbf{r}_2 \tilde{\rho}(\mathbf{r}_1) \tilde{\rho}(\mathbf{r}_2) |\mathbf{r}_1 - \mathbf{r}_2| \\ &= \frac{1}{2} k \int 4\pi r_1^2 dr_1 \tilde{\rho}(r_1) \int 2\pi r_2^2 \tilde{\rho}(r_2) \sqrt{r_1^2 + r_2^2} \times \end{aligned}$$

$$\begin{aligned}
& \int d \cos \theta \sqrt{1 - q \cos \theta} \\
= & \frac{8\pi^2}{3} kR \int \int d\bar{r}_1 d\bar{r}_2 \bar{r}_1^2 \bar{r}_2^2 \tilde{\rho}(\bar{r}_1) \tilde{\rho}(\bar{r}_2) \sqrt{\bar{r}_1^2 + \bar{r}_2^2} \times \\
& \left[(1+q)^{3/2} - (1-q)^{3/2} \right].
\end{aligned} \tag{A17}$$

Evaluated over a Bonnor-Ebert sphere,

$$\langle \sigma^2 \rangle^{1/2} = 0.607 k^{1/2} R^{1/2}, \tag{A18}$$

and in combination with equation (A5),

$$\langle j^2 \rangle^{1/2} = 0.414 \langle \sigma^2 \rangle^{1/2} R. \tag{A19}$$

Since the velocity distribution is Gaussian, all of its linear moments (e.g., L_x and σ) are Gaussian distributed. The cumulative probability distribution of j , $\mathcal{P}(< j)$, is therefore Maxwellian with a width fixed by equation (A19):

$$\frac{d\mathcal{P}(< j)}{d(j/\langle j^2 \rangle^{1/2})} = 3\sqrt{\frac{6}{\pi}} \frac{j^2}{\langle j^2 \rangle} \exp\left(-\frac{3j^2}{2\langle j^2 \rangle}\right) \tag{A20}$$

A log-normal fit to this distribution is $\log_{10} j/\langle j^2 \rangle^{1/2} = -0.080 \pm 0.52$, but this is not especially accurate. A more faithful representation is $\log_{10} j/\langle j^2 \rangle^{1/2} = -0.088_{-0.49}^{+0.16}$.